

Th-234 Scavenging in the Water Column off Southwestern Taiwan

CHIN-CHANG HUNG AND CHING-LING WEI

ABSTRACT

A station off southwestern Taiwan (22° 25'N 120° 08'E) was selected to carry out detailed seawater sampling for the measurements of dissolved and particulate ^{234}Th . The profiles showed that ^{234}Th is subject to scavenging and removal processes by biological particles in the euphotic zone and by resuspended particles in the deep layer. Estimated by box-model, the residence times of dissolved and particulate ^{234}Th in the euphotic layer are in the ranges of 90–110 days and 12–28 days, respectively. A vertical ^{234}Th flux of $1220 \text{ dpm m}^{-2} \text{ d}^{-1}$ out of the euphotic layer is estimated. Horizontal transport of resuspended particles in the deep and bottom layer is evident based on morphological examination of particles but is difficult to quantify. Resuspended particles act as an effective scavenger for Th in the deep layer and cause a radioactive disequilibrium of ^{234}Th with respect to its progenitor, ^{238}U . Residence times of dissolved and particulate ^{234}Th in this layer are 112 days and 35 days, respectively. A lower limit of ^{234}Th flux of $1600 \text{ dpm m}^{-2} \text{ d}^{-1}$ into the bottom sediment can be estimated.

1. INTRODUCTION

It is well-known that 'particle-reactive' elements are subject to scavenging onto particle surface and removed from the ocean via particle settling (Goldberg, 1954). As radionuclides are measured in both dissolved and particulate phases, we are able to estimate not only how fast the elements are scavenged but also the settling velocity of particulate matter in the water column. The power of radionuclides originates from its definite decay rate which provides a 'clock' for the processes which govern the distribution of elements in the ocean.

Compatible time scale of radioactive life time of ^{234}Th (34.8 days) and the residence time of marine particulate matter have made ^{234}Th a very useful tracer in studying scavenging phenomena in the upper layer of the open ocean (Bhat, 1969; Bacon and Anderson, 1982; Coale and Bruland, 1985, 1987; Bruland and Coale, 1986; Murray *et al.*, 1989; Buesseler *et al.*, in press) and in coastal waters (Minagawa and Tsunogai, 1980;

Kaufman *et al.*, 1981; McKee *et al.*, 1984, 1986; Coale and Bruland, 1985; Wei and Murray, 1991, 1992).

Compared to the open ocean, coastal waters have enhanced scavenging properties and more dynamic characteristics of particle cycling. This is because terrestrial input of particulates and resuspended sediments play a significant role in scavenging processes. In this paper, we investigated the scavenging processes of ^{234}Th in a station about 22.5 km off Kaohsiung Harbor. We have determined detailed vertical profiles of dissolved and particulate ^{234}Th in the water column. Scavenging and particle removal rates will be estimated using a box model calculation.

2. METHOD

Seawater samples were collected at the station (22° 25'N 120° 08'E, water depth=580 m) during 26 December 1991, onboard R/V Ocean Researcher I (cruise # 306a). A CTD/2.5 l Niskin system attached with a fluorescence sensor was used to obtain hydrographic data (T, S, dissolved oxygen, NO_3 , NO_2 , PO_4 , and SiO_2). Large volume seawater casts for radionuclides determination were executed by separate hydrocast. About 20 liters of seawater were collected using 20 l Go-Flo bottles mounted on hydrowire. Seawater was immediately pressure-filtered by compressed air through a pre-weighed 142 mm Nuclepore filter (0.45 μm) mounted in a Plexiglas filter holder.

After filtration, the filter was rinsed with about 10 ml deionized distilled water and stored in a petri dish and returned to the laboratory. Preconcentration and separation of uranium and thorium from the filtered seawater samples were carried out on board ship. Detailed procedures for ^{234}Th sample handling can be found in Wei and Murray (1991, 1992) and Wei and Hung (1992). During this cruise, parallel samples for dissolved and particulate ^{210}Pb and ^{210}Po determinations were also collected. Particulates collected by Nuclepore filters were examined using the scanning electron microscope (JSM-5400). The ^{210}Pb and ^{210}Po results along with particulate composition will be reported in a separate paper (Wei *et al.*, in prep.).

The activities of ^{234}Th were counted by a low background (<0.3 cpm) anticoincidence counter (Tennelec LB-5100) via its β -emitting daughter ^{234}Pa . The purity of samples was checked by counting through a time span of about two months to confirm that the radioactive decay curve was followed (Wei, 1991). Blank determinations of all reagents and filter paper used for this study indicated negligible contribution. Chemical yield of thorium was estimated by counting spiked ^{230}Th using silicon surface-barrier detectors (EG&G Ortec 576). The counting efficiencies of the detectors were calibrated against NIST traceable ^{241}Am (Isotope Products Laboratory 387-67-2-2) and ^{230}Th (Isotope Products Laboratory 387-67-3) standard plates. Activities of ^{234}Th reported here were corrected back to the sampling time after the ingrowth of ^{234}Th from ^{238}U was subtracted.

3. RESULTS

Depth, salinity, calculated ^{238}U activities, concentrations of total suspended matter (TSM), dissolved (DTh) and particulate (PTh) ^{234}Th activities are given in Table 1. Uncertainties of all radioisotope data listed were estimated according to the propagation of counting error ($\pm 1\sigma$). Hydrographic and nutrients data are not listed but are available upon request.

The vertical distributions of hydrographic data (salinity, temperature, and potential density), fluorescence and TSM concentration, and dissolved oxygen and nutrients (PO_4 , NO_3 , NO_2 , and SiO_2) at the sampling station are shown in Figures 1-3, respectively. Dissolved and particulate ^{234}Th with counting error bars are shown in Figure 4. Total ^{234}Th activities as the sum of dissolved and particulate ^{234}Th are also included in the figure. A dotted line drawn at 2.39 dpm kg^{-1} in the figure represents ^{238}U activity calculated from the S- ^{238}U relationship from Ku *et al.* (1977).

It is evident from interleaving salinity structure (Figure 1) that the water column is subject to complicated water mixing. A minimum of 34.2 psu and a maximum of 34.8 psu were found at the depth of 40 m and 125 m, respectively. Several interfingering structures were observed in the upper 200 m. The salinity maximum is caused by intrusion of the Kuroshio (Shaw, 1989). Main pycnocline of $0.05 \sigma_\theta \text{ m}^{-1}$ was in the layer of 95–125 m and a secondary pycnocline of $\sim 0.007 \sigma_\theta \text{ m}^{-1}$ was in the layer of 125–325 m. Nutrients

Table 1. Depth, salinity, calculated ^{238}U , total suspended matter (TSM) concentration, dissolved and particulate ^{234}Th collected in 26 December 1991. Standard deviations are based on propagated counting error ($\pm 1\sigma$).

Depth m	Salinity psu	^{238}U dpm kg^{-1}	TSM mg kg^{-1}	Diss. ^{234}Th dpm kg^{-1}	Part. ^{234}Th dpm kg^{-1}
0	34.536	2.380	0.22	1.274 ± 0.098	0.311 ± 0.018
5	34.520	2.379	0.11	1.767 ± 0.115	0.263 ± 0.014
10	34.517	2.379	0.10	1.914 ± 0.085	0.258 ± 0.014
20	34.440	2.373	0.13	1.648 ± 0.066	0.362 ± 0.016
30	34.357	2.368	0.14	1.731 ± 0.078	0.212 ± 0.011
50	34.316	2.365	0.13	1.970 ± 0.103	0.072 ± 0.004
100	34.643	2.387	0.06	1.604 ± 0.132	0.186 ± 0.012
150	34.789	2.397	0.04	2.168 ± 0.093	0.361 ± 0.019
200	34.720	2.393	0.04	2.226 ± 0.095	0.210 ± 0.012
250	34.629	2.386	0.12	1.868 ± 0.078	0.155 ± 0.007
300	34.579	2.383	0.14	1.561 ± 0.073	0.301 ± 0.018
400	34.501	2.378	0.07	2.490 ± 0.109	0.327 ± 0.030
500	34.501	2.378	0.34	2.076 ± 0.074	0.323 ± 0.019

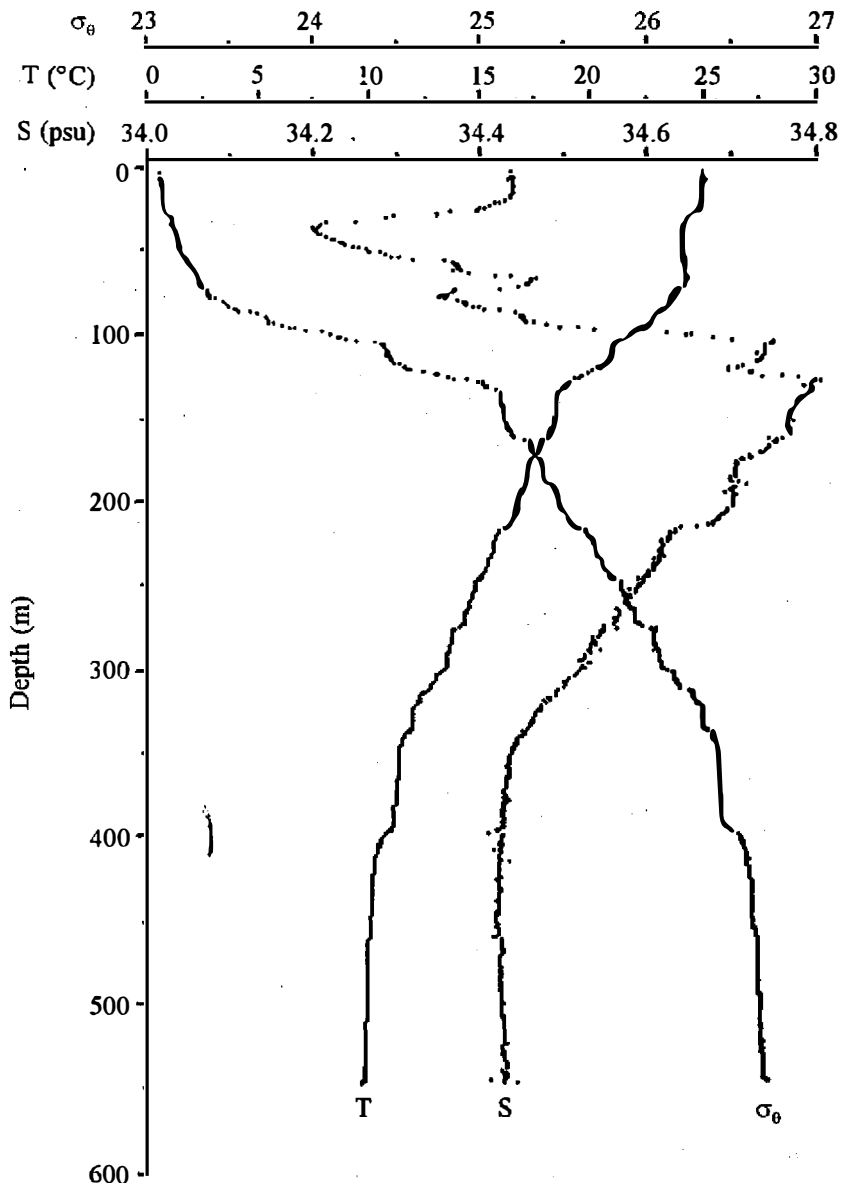


Fig. 1. Vertical profiles of temperature, salinity, and potential density.

were depleted in the mixed layer then increased with depth in the pycnocline layer (Figure 2). A sharp nitrite maximum of $0.43 \mu\text{M}$ centered at 100 m was observed. Dissolved oxygen decreased from saturation level in the mixed layer to $185 \mu\text{M}$ at S maximum. It should be noted that the sharpest gradient of dissolved oxygen was found in the upper pycnocline where nutrients increases abruptly. Below 200 m depth, dissolved oxygen continued to decrease and nutrients showed monotonically increasing trend toward the bottom.

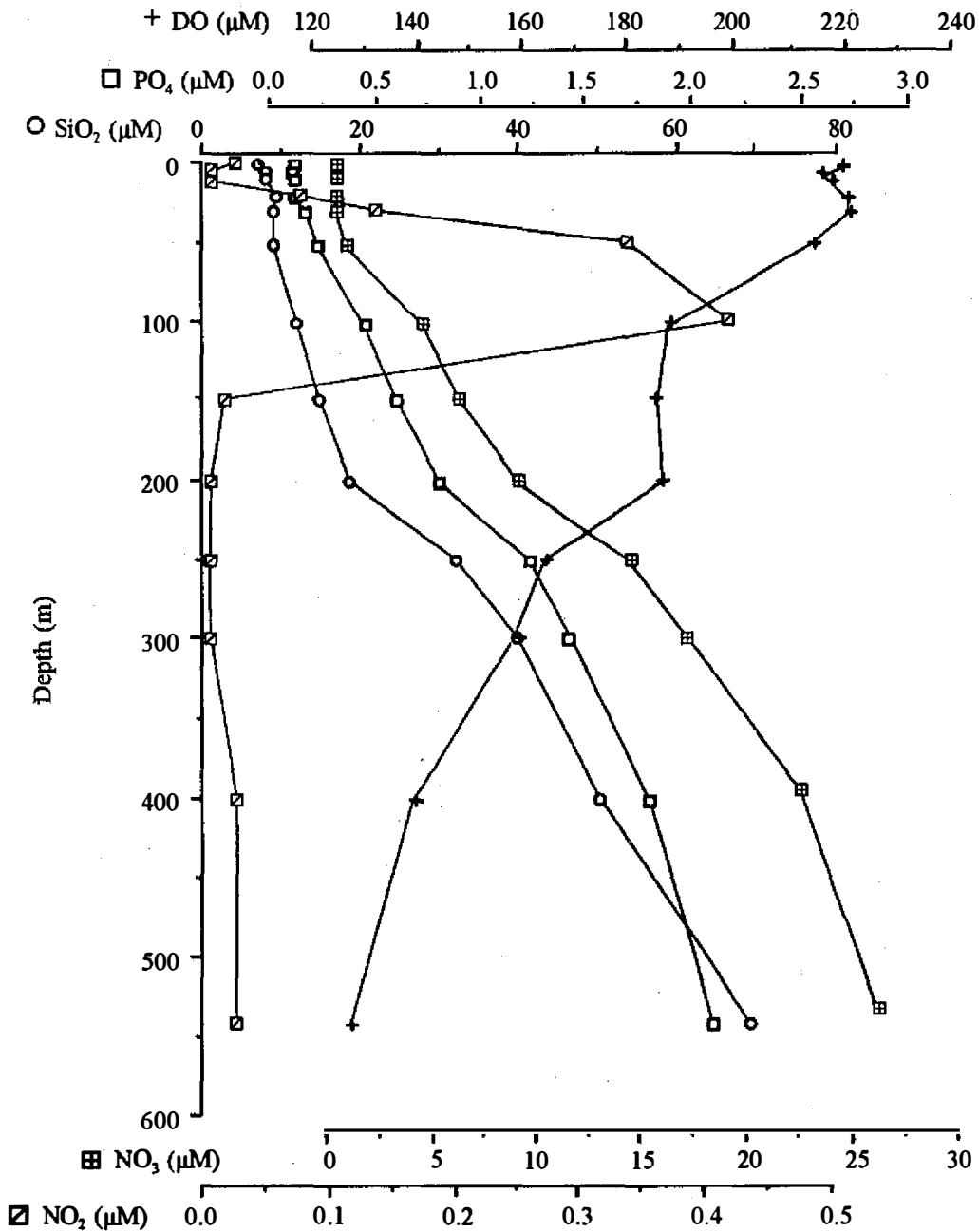


Fig. 2. Vertical profiles of dissolved oxygen, phosphate, silicate, nitrate, and nitrite.

A sharp fluorescence peak was observed at 38 m. The fluorescence signal diminished to its background value at the depth of about 135 m. In Figure 3, TSM concentrations were overlapped with the fluorescence for comparison. TSM was enriched in the mixed layer then dropped to ~0.15 mg kg⁻¹ at the base of upper pycnocline. In the upper 135 m,

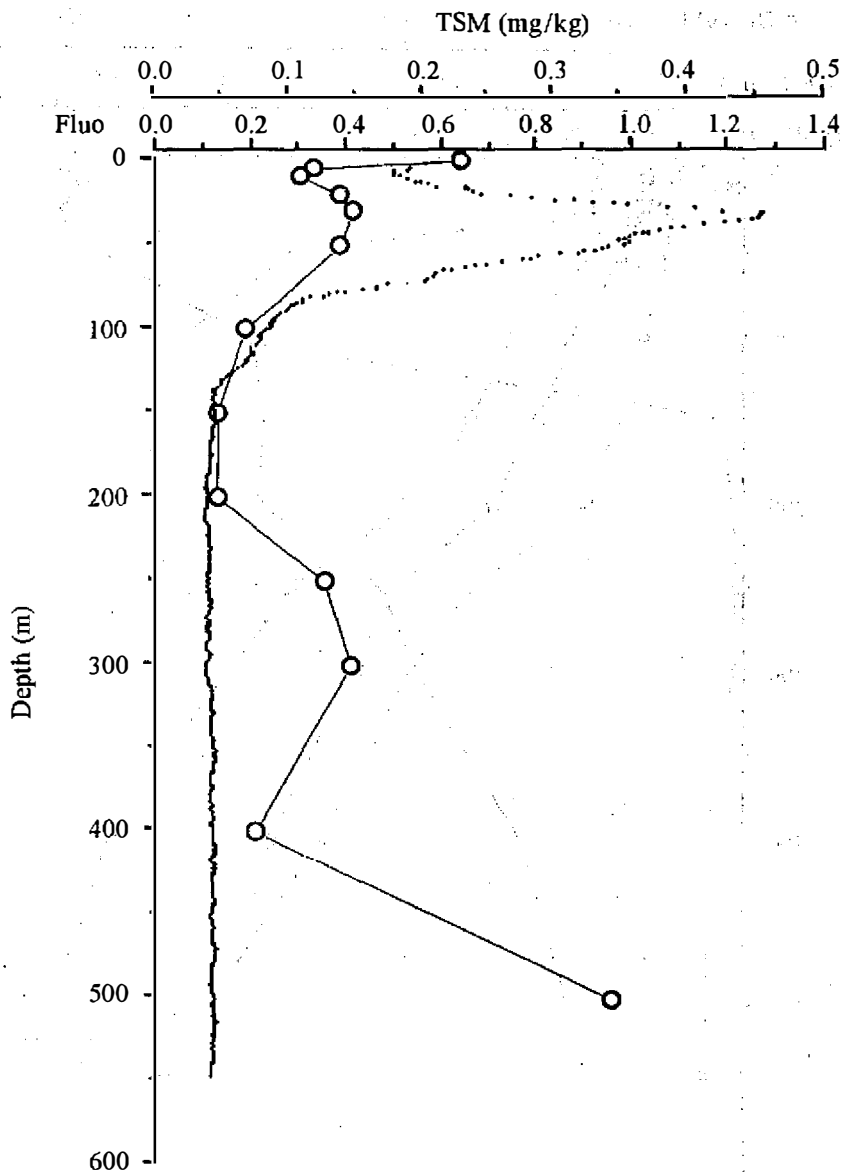


Fig. 3. Vertical profiles of fluorescence and total suspended matter (TSM) concentration.

the shape of vertical profiles of TSM and fluorescence were remarkably similar, which indicated that particles caught by the filters in the upper water column were dominated by biological particles. The pictures of scanning electron microscope on the filters showed that planktons were the major phases of the particles in the upper 200 m (Wei *et al.*, in prep.). An evident particle-enriched layer, with TSM concentration of 0.4 mg kg^{-1} , was observed in the depth of 250–350 m, which should be caused by horizontal input of resuspended sediments. Our interpretation of this deep TSM maximum is supported by

the direct SEM examination of the particles which are dominated by detritus of aluminosilicate minerals.

Figure 4 shows that all dissolved ^{234}Th except at 400 *m* were deficient relative to the secular equilibrium values. Maximal deviations of dissolved ^{234}Th from ^{238}U were found in the photic zone and in the deep TSM maximum layer. Particulate ^{234}Th in the euphotic layer showed mirror image of dissolved ^{234}Th . A minimum of particulate ^{234}Th of only 0.1 dpm kg^{-1} was located at S minimum layer. Total ^{234}Th profile was similar to dissolved profile because dissolved form was the dominant phase of ^{234}Th in seawater.

4. BOX MODEL FOR ^{234}Th SCAVENGING

The most commonly used model for ^{234}Th scavenging in the water column of the ocean is the irreversible scavenging model (Coale and Bruland, 1985, 1987; Wei and Murray, 1991, 1992). As pointed out by Wei and Murray (1992), the scavenging and particle removal rates can be calculated either by a point-by-point approach or by dividing the water column into a number of boxes then carrying out a mass balance calculation. Here we adopted the box model approach. The water column was divided into five boxes based on the vertical stability. The four boundaries between boxes were 20 *m*, 100 *m*, 220 *m*, and 345 *m*. In each box, inventories of dissolved and particulate ^{234}Th were calculated from either measured or linearly interpolated values. Assuming steady state and negligible effect of physical mixing, two mass balance equations can be established for dissolved and particulate ^{234}Th , respectively.

$$J_i = \lambda U_i - \lambda DTh_i \quad (1)$$

$$F_i = J_i - \lambda PTh_i + F_{i-1} \quad (2)$$

where

U_i, DTh_i, PTh_i = inventories of ^{238}U , dissolved ^{234}Th , particulate ^{234}Th in dpm m^{-2} in box *i*, respectively,

J_i, F_i = scavenging and vertical fluxes ($\text{dpm m}^{-2} \text{d}^{-1}$) in and from box *i*,

λ = radioactive decay constant of ^{234}Th (0.0288 d^{-1}), and

i = integers from 1 to 5.

Residence times for dissolved (τ_{DTh}) and particulate (τ_{PTh}) ^{234}Th relative to scavenging and particulate fluxes in each box can be calculated by :

$$\tau_{DTh_i} = \frac{DTh_i}{J_i} \quad (3)$$

$$\tau_{PTh_i} = \frac{PTh_i}{F_i - F_{i-1}} \quad (4)$$

The results of box model calculation are shown in Figure 5.

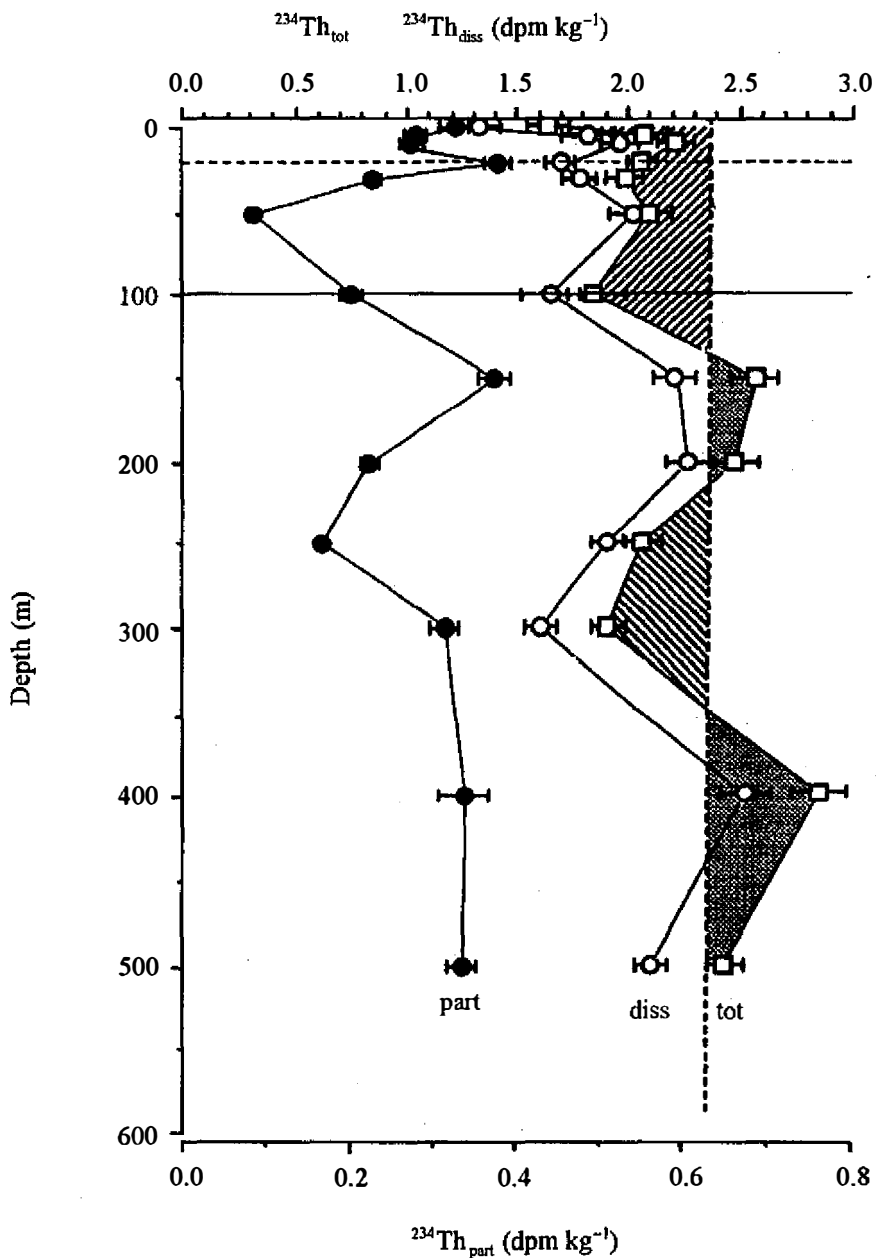


Fig. 4. Vertical profiles of total, dissolved and particulate ^{234}Th . The vertical dashed line at 2.39 dpm kg^{-1} represents ^{238}U activity calculated from S- ^{238}U relationship. Error bars represent uncertainties based on propagated counting error. The bases of mixed depth and euphotic zone are shown as the horizontal dashed and solid lines, respectively. Deficiencies and excesses of total ^{234}Th relative to ^{238}U are shown as hatched and grey area, respectively.

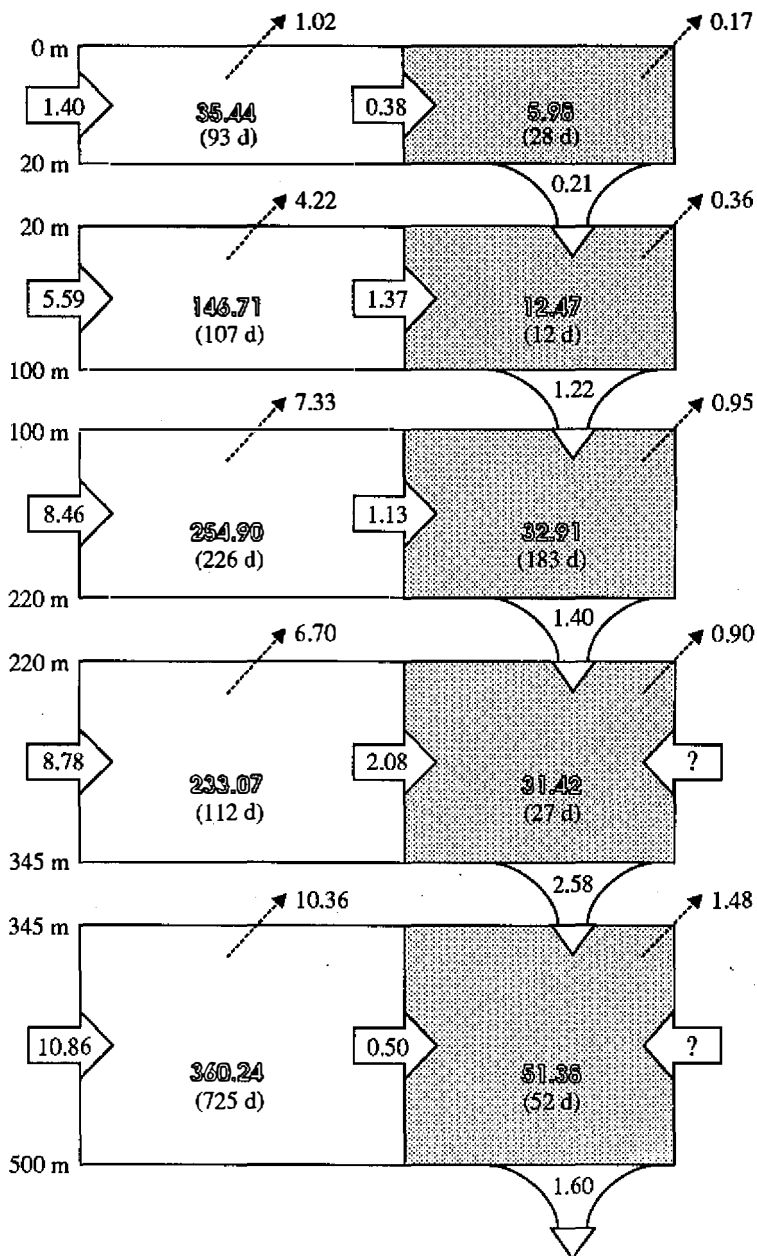


Fig. 5. Results of box-model calculation from equations (1) to (4). Inventories of dissolved (blank box) and particulate (grey box) ²³⁴Th are written as outlined characters in unit of 1000 dpm m⁻². Numbers in bracket are residence times in day. Horizontal arrows into the dissolved (particulate) ²³⁴Th boxes are production (scavenging) fluxes from ²³⁸U (dissolved ²³⁴Th). Dashed arrows are fluxes of radioactive decay. Vertical arrows represent fluxes of ²³⁴Th via particle settling from overlying boxes. All fluxes are in unit of 1000 dpm m⁻² d⁻¹.

5. DISCUSSIONS

5.1 Implication of particle dynamics in the euphotic layer

Euphotic layer is a unique system in which biological materials are produced, recycled and then transported into the interior of the ocean. One of the primary goals of JGOFS (Joint Global Ocean Flux Study) is to quantify the export flux of carbon out of the euphotic zone. Th-234 has been identified to be a superior tracer for particulate organic carbon (Eppley, 1989; U.S. JGOFS Report # 12, 1990) to estimate the export production. The rationale of this recommendation is based on the findings that ^{234}Th scavenging responds to primary productivity (Coale and Bruland, 1985) and to organic particulate flux (Bruland and Coale, 1986). Furthermore, the residence time of POC with respect to its production rate in the euphotic layer is similar to that of ^{234}Th , which makes ^{234}Th a potential tracer for biological particles (Wei and Murray, 1992). Recently, Beals and Bruland (in press) found that dissolved ^{234}Th residence time inversely correlates with fluorescence in the Northeast Pacific Ocean. All of these findings warrant obtaining more ^{234}Th data on both spatial and temporal bases.

Nutrient measurements showed that the surface water at the site was a NO_3 -limiting system (Figure 2). NO_3 concentration in the mixed layer was below the detection limit ($0.3 \mu\text{M}$) then started to increase at the base of the mixed layer. Other nutrients (PO_4 and SiO_2) showed a similar increasing trend but the surface concentrations never diminished to detection limit values. At this specific region, the euphotic depth was at 100 m, about 75 m deeper than the mixed depth. Such euphotic system (euphotic depth > mixed depth) is commonly found in meso- and oligotrophic pelagic oceans and is called stratified two-layer system (Dugdale, 1967).

The impact of the two-layer euphotic structure on ^{234}Th scavenging was studied by Coale and Bruland (1987). In the mixed layer off Mexico, the productivity was fueled by regenerated nutrients, and planktonic community was dominated by pico- or nanoplanktons. In this oligotrophic mixed layer, ^{234}Th was scavenged onto particles but not readily transported out of the mixed layer because the particles in it were small in size, and decomposition rate of particles might be relatively fast compared to the long residence time of particles. On the other hand, the lower euphotic layer was a lit system with relatively high nutrients. Thus, the productivity was mainly supported by nitrate and the planktons which resided in it were larger in size. The export fluxes of ^{234}Th out of this layer were high because of fast scavenging and repackaging rates.

At our sampling station, dissolved ^{234}Th in the mixed layer were not significantly higher than those in the lower euphotic layer. Particulate ^{234}Th was higher in the mixed layer than those in the lower euphotic zone by $\sim 0.2 \text{ dpm kg}^{-1}$. The sum of dissolved and particulate ^{234}Th (total ^{234}Th) between two layers was not as contrasted as the case found off Mexico (Coale and Bruland, 1987). Lack of clear two-layered Th structure at the station implies that ^{234}Th dynamics in the euphotic zone was not as simple as we thought.

A clear picture of trophic dynamics in the euphotic zone in different oceanographic regimes must be known.

A subsurface chlorophyll maximum (SCM) was observed at the base of the mixed layer. At the SCM, dissolved ^{234}Th showed evident minimum values and TSM concentrations showed maximal values. The association of SCM and dissolved ^{234}Th minimum was consistent with the case found in the Northeast Pacific Ocean (Beals and Bruland, in press), which confirmed the close relationship of ^{234}Th scavenging and biological activities. Residence time and fluxes of ^{234}Th in the euphotic layer can be calculated from the degree of disequilibrium and will be presented in the following section.

5.2 Implication from excessive ^{234}Th in the deep layers

It is noted that four (150, 200, 400, and 500 m) out of thirteen samples had excessive total ^{234}Th relative to ^{238}U (Figure 4). Excessive ^{234}Th relative to ^{238}U was also observed by others. In the profiles of Coale and Bruland (1987), excessive total ^{234}Th over ^{238}U was found below the euphotic layer at two stations in the North Pacific Ocean. In the Panama Basin, total ^{234}Th activities exceed ^{238}U at certain depths (Murray *et al.*, 1989). However, the extent of excess was too small, usually in the range of uncertainty, to confirm if the excess signal was real.

Judging from the relatively large difference between total ^{234}Th and ^{238}U at our sampling station, we believe the excess signal is a real feature. The excessive ^{234}Th over ^{238}U at aforementioned depths may be due to particle regeneration and/or retardation of particle settling. It can be seen from Figure 4, dissolved ^{234}Th approaches ^{238}U at these depths, implying that regeneration of ^{234}Th is a slow process relative to the radioactive turn-over rate of ^{234}Th . Although representing a small pool (~10%), particulate phase plays a major role in the exchange of ^{234}Th between different layers. It is interesting that the particulate ^{234}Th above the ^{234}Th -excess layers are usually smaller than those in other depths. Accordingly, the layers with enriched ^{234}Th may be caused by 'trapping' effect on settling particles originated from the overlying layers.

5.3 Importance of horizontal transport of resuspended particles

A significant deficiency of ^{234}Th with respect to ^{238}U by ~ 0.5 dpm kg^{-1} was observed at depths of 250 and 300 m. In these depths, TSM concentration reached a maximum of 0.15 mg kg^{-1} (Figure 3). We believe that the disequilibrium of ^{234}Th and ^{238}U was caused by horizontal injection of resuspended particles from the continental slope. Because of the short radioactive lifetime of ^{234}Th , the turn-over rate of ^{234}Th is relatively fast so that the disequilibrium below the euphotic layer is seldom found in the open ocean. An exception of this is coastal regime (i.e., Dabob Bay, Washington, USA, Wei and Murray, 1992) where the water depth is shallow and resuspension of bottom sediments is effective in removing ^{234}Th from seawater.

Direct evidence of the horizontal transport of resuspended particles was detrital composition from SEM examination of filtered particles collected at these depths. Over 95% of particulates at these depths were detritus material (Wei *et al.*, in prep). The specific activity of ^{234}Th in the bottom sediments may be lower than that in the suspended particles, hence, acting as an effective Th scavenger when resuspended in the water column (Wei and Murray, 1992).

5.4 Inferences from box-model

The water column was divided into five boxes and can be envisioned as upper euphotic, lower euphotic, intermediate and two bottom boxes. Each box has its own characteristics which determine the scavenging and removal rates. For example, the upper euphotic box (box 1) is characterized by low nutrient, high phytoplankton population, high regenerated productivity, and low POC flux. The lower euphotic box (box 2) is characterized by high nutrients, lower phytoplankton population, high new productivity, and high POC flux. In the two bottom boxes (boxes 4 and 5) suspended particles are dominated by detritus materials which may impose a rather different scavenging force for ^{234}Th .

Figure 5 summarized the fate of ^{234}Th in the water column. The common feature shared by different boxes is that τ_{DTh} is always longer than τ_{PTh} , implying that uptake/adsorption rate controls the non-radioactive sink for ^{234}Th at the station. In evident ^{234}Th -deficiency layers (box 1, 2, 4), τ_{DTh} is about 100 days while in other layers τ_{DTh} is too long to be resolved by the disequilibrium. τ_{PTh} ranges from 12 days associated with the lower euphotic box (box 2) to 183 days associated with the intermediate box (box 3), giving an average settling velocity from 0.7 m d^{-1} to 6.7 m d^{-1} .

Comparing with the other area, residence time of dissolved ^{234}Th , 100 days, in the euphotic layer of the station is long. In the coastal California Current, the τ_{DTh} ranges from 6 to 47 days (Coale and Bruland, 1985). Recently, Wei and Hung (1992) found that τ_{DTh} in the surface water of the Bashi Channel and the Luzon Strait is also short, mostly shorter than 50 days. The surface water of the Bashi Channel has the same source of water as the study area (Shaw, 1989). The abnormally long τ_{DTh} in the area should be related to low local biological productivity. Unfortunately, there is no primary productivity data to confirm the interpretation.

Vertical fluxes of ^{234}Th estimated from the box-model range from 210 to $2580 \text{ dpm m}^{-2} \text{ d}^{-1}$, and generally increase with depth except the bottom box. It should be pointed out that the estimated ^{234}Th fluxes from the two bottom boxes are lower limits. This is because a horizontal input of resuspended sediments, evident from dominant detrital materials on the filters (Wei *et al.*, in prep), was not considered. If this component was known and included in the mass balance equation (eq. (2)), a higher vertical ^{234}Th flux should be expected. Unfortunately, a quantitative determination of the input was difficult to make; hence, we put a question mark on the box and interpreted the results with caution.

It is informative to compare the magnitudes of scavenging flux (J) and vertical flux (F). From boxes 1 to 5, the ratios of J and F are 1.81, 1.12, 0.81, 0.81, and 0.31, respectively. The ratios indicate that most of the vertical ^{234}Th fluxes in the euphotic boxes (box 1 and 2) originate from scavenging of dissolved ^{234}Th onto particulate materials, while only a small proportion of vertical ^{234}Th flux in the bottom box (box 5) is contributed from scavenging.

6. SUMMARY

A detailed study of dissolved and particulate ^{234}Th in the water column of a station off southwest Taiwan has enabled us to assess the scavenging and particle removal processes. The water column under investigation has a stratified two-layer euphotic layer and a deep layer subjected to the influence of active horizontal input of resuspended sediments. Pronounced deficiencies of ^{234}Th relative to ^{238}U in the euphotic and deep layers were observed. On the other hand, a significant amount of excessive ^{234}Th was found below the euphotic zone and in the bottom water, which is caused by regeneration and/or trapping effect of settling particles. We adopted a box-model to estimate the residence times of dissolved and particulate ^{234}Th . Furthermore, vertical fluxes of ^{234}Th out of five compartments were also estimated.

Acknowledgments We are indebted to Mr. Gwo-Ching Gong and his hydrographic group for measuring nutrients and dissolved oxygen. Dr. M.-P. Chen helped us in SEM examination of filtered particles. We would also like to thank the crew of the Ocean Researcher I for their assistance with the sample collection. This study was supported by the National Science Council under grants NSC80-0209-M002a-13 and NSC-81-0209-M002a-06.

REFERENCES

- Bacon, M. P. and R. F. Anderson, 1982: Distribution of thorium isotopes between dissolved and particulate forms in the deep sea, *J. Geophys. Res.*, **87**, 2045–2056.
- Beals, D. and K. W. Bruland (in press) Scavenging of Th-234 in the Pacific Ocean. *Deep-Sea Res.*
- Bhat, S. G., S. Krishnaswami, D. Lal, Rama, and W. S. Moore, 1969: $^{234}\text{Th}/^{238}\text{U}$ ratios in the ocean, *Earth Planet. Sci. Lett.* **5**, 483–491.
- Bruland, K. W. and K. H. Coale, 1986: Surface water $^{234}\text{Th}/^{238}\text{U}$ disequilibria: Spatial and temporal variations of scavenging rates within the Pacific Ocean, in J. D. Burton, P. G. Brewer, and R. Chesselet (eds.) *Dynamic Processes in the Chemistry of the Upper Ocean*. Plenum Pub. Co., pp. 159–172.
- Buesseler, K. V., M. P. Bacon, J. K. Cochran, and H. D. Livingston (in press) Carbon and nitrogen export during the JGOFS North Atlantic Bloom Experiment estimated from

- $^{234}\text{Th}/^{238}\text{U}$ disequilibria. *Deep-Sea Res.*
- Coale, K. H. and K. W. Bruland, 1985: $^{234}\text{Th}/^{238}\text{U}$ disequilibria within the California Current. *Limnol. Oceanogr.* **30**, 22–33.
- Coale, K. H. and K. W. Bruland, 1987: Oceanic stratified euphotic zone as elucidated by $^{234}\text{Th}/^{238}\text{U}$ disequilibria. *Limnol. Oceanogr.* **32**, 189–200.
- Dugdale, R. C., 1967: Nutrient limitation in the sea: Dynamics, identification and significance. *Limnol. Oceanogr.* **12**, 685–695.
- Eppley, R. W., 1989: New production: history, methods and problems. In: Dahlem Workshops in "Productivity of the Ocean: Present and Past". W. H. Berger, V. Smetacek, and O. Weffer (eds.), Wiley, New York, pp. 85–97.
- Goldberg, E. D., 1954: Marine Chemistry I. Chemical scavengers of the sea. *J. Geol.*, **62**, 249–265.
- Ku, T. L., K. G. Knauss, and G. G. Mathiew, 1977: Uranium in open ocean: concentration and isotopic composition. *Deep-Sea Res.* **24**, 1005–1017.
- McKee, B. A., D. J. DeMaster, and C. A. Nittrouer, 1984: The use of $^{234}\text{Th}/^{238}\text{U}$ disequilibrium to examine the fate of particle-reactive species on the Yangtze continental shelf. *Earth Planet. Sci. Lett.* **68**, 431–442.
- McKee, B. A., D. J. DeMaster, and C. A. Nittrouer, 1986: Temporal variability in the partitioning of thorium between dissolved and particulate phases on the Amazon shelf: implications for the scavenging of particle-reactive species. *Cont. Shelf Res.* **6**, 87–106.
- Murray, J. W., J. N. Downs, S. Strom, C.-L. Wei, and H. W. Jannasch, 1989: Nutrient assimilation, export production and ^{234}Th scavenging in the Eastern Equatorial Pacific. *Deep-Sea Res.*, **36**, 1471–1489.
- Shaw, P.-T., 1989: The intrusion of water masses into the sea southwest of Taiwan. *J. Geophys. Res.*, **94**, 18213–18226.
- U.S. JGOFS, 1990: Isotopic tracers. U.S. JGOFS Planning Report # 12. Woods Hole Oceanographic Institution. 116pp.
- Wei, C.-L., 1991: Studies of scavenging phenomenon in the upper water column off Northeast Taiwan – Application of $^{234}\text{Th}/^{238}\text{U}$ disequilibrium. *Acta Oceanographica Taiwanica*, **26**, 13–19.
- Wei, C.-L. and C.-C. Hung (in press) Spatial variation of ^{234}Th scavenging in the surface water of the Bashi Channel and the Luzon Strait. *J. Oceanogr.*
- Wei, C.-L. and J. W. Murray, 1991: $^{234}\text{Th}/^{238}\text{U}$ disequilibria in the Black Sea. *Deep-Sea Res.*, **38**, s855–s873.
- Wei, C.-L. and J. W. Murray, 1992: Temporal variation of ^{234}Th activity in the water column of Dabob Bay: Particle scavenging. *Limnol. Oceanogr.*, **37**, 296–314.
- Wei, C.-L., C.-C. Hung and M.-P. Chen (in prep) Comparative geochemistries of ^{234}Th , ^{210}Pb , and ^{210}Pb in the water column off southwestern Taiwan.

台灣西南海域水體中 T-234 的清除作用

洪慶章 魏慶琳
台灣大學海洋研究所

摘 要

本研究於台灣西南海域選擇一測站 (22°25'N 120°08'E)，採集海水以量測溶解相及顆粒相鈷-234。自垂直剖面觀之，鈷-234 在透光層主要是受生物活動，深層則是被再懸浮顆粒所清除。於透光層中，由盒子模式計算溶解相與顆粒相鈷-234 之停留時間分別為 90-110 天和 12-28 天；並據以推算鈷-234 在透光層底部的通量為 1220 dpm m⁻²d⁻¹。從顆粒的外形鑑定，顯示深層及底層之顆粒體為水平方向傳送過來之再懸浮顆粒組成，但難以定量。再懸浮顆粒體為一有效之鈷-234 清除者，造成深層水中鈷-234 和鈾-238 之不平衡。在深層水中，溶解相和顆粒相鈷-234 之停留時間分別為 112 天和 27 天。我們估計鈷-234 進入沉積物中之最低通量為 1600 dpm m⁻²d⁻¹。